

## THE MOLECULAR CLOUD COMPLEX ASSOCIATED WITH ON 1

F. P. ISRAEL

Astronomy Division, Space Science Department, ESA, ESTEC; and Goddard Institute for Space Studies

AND

H. A. WOOTTEN

Owens Valley Radio Observatory

Received 1982 February 4; accepted 1982 August 27

### ABSTRACT

Observations of CO with different resolutions near the compact H II region/maser source ON 1 are presented, as well as new H<sub>2</sub>CO and HCO<sup>+</sup> observations. ON 1 is part of an extended molecular cloud complex with overall dimensions of 25×60 pc at a distance of 1.4 kpc; it appears to be the only site of star formation in at least the western part of the complex. ON 1 coincides with a compact and dense molecular cloud core (size 0.8 pc) that shows little sign of disruption indicating that ON 1 has only recently turned on. The isolation and apparent youth of ON 1 suggest that we observe here the very beginning of the star formation phase of a molecular cloud complex.

*Subject headings:* interstellar: molecules — masers — nebulae: H II regions — stars: formation

### I. INTRODUCTION

One of the first main line OH masers discovered that is not associated with a strong radio continuum source was the object ON 1 (Elldér, Rönnäng, and Winnberg 1969; see also Cohen and Willson 1981; Lunel *et al.* 1980), situated at the edge of the heavily obscured Cygnus Rift region in the Milky Way. Subsequent radio continuum observations by Winnberg, Habing, and Goss (1973) led to the discovery of a coincident ultracompact H II region with an emission EM =  $3 \times 10^8$  pc cm<sup>-6</sup>. A highly variable H<sub>2</sub>O maser was likewise found near ON 1 (Cato *et al.* 1976; see also Genzel and Downes 1977; Downes *et al.* 1979). Lunel *et al.* (1980) have mapped the region in the near-infrared and described a source, IRS 1, which lies very near the OH/H<sub>2</sub>O position. Thus, the ON 1 object marks the site of very recent star formation.

Although the Great Cygnus Rift is very poorly covered by radio continuum surveys, the aperture synthesis observations by Winnberg, Habing, and Goss (1973) established that ON 1 is an isolated object; no radio continuum emission other than that due to the ultracompact object is evident in their 21 cm map. In this respect ON 1 appears indeed to be unique: almost all other known compact and ultracompact H II regions are found in the vicinity of other compact or extended H II regions (Israel 1976; Habing and Israel 1979). Therefore, one may speculate that ON 1 represents a case of first-generation star formation.

This consideration prompted us to conduct an extensive study of the neutral surroundings of ON 1 in several molecular lines. In order to set the stage, we will first

discuss a large scale CO map of the ON 1 area. This is followed by a discussion of the molecular cloud that is associated with ON 1 itself, whose core was observed in a variety of molecular lines at different transitions.

### II. OBSERVATIONS

#### a) CO Observations at Columbia

An extended area, measuring roughly 2°×2°, was fully mapped using the Columbia University 1.2 m millimeter-wavelength telescope in New York City. This telescope has a beamwidth (FWHM) of 8' at the observing frequency of 115 GHz and a beam efficiency of 70%. Intensity is given in units of  $T_A^*$ , equivalent to the  $T_R^*$  defined by Kutner and Ulich (1981). At the time of the observations (1976 March), the receiver had a single-sideband total system noise temperature of about 1500 K. The spectrometer had a total bandwidth of 40 MHz, while a 40-channel filter-bank provided a spectral resolution of 1 MHz (corresponding to a velocity resolution of 2.6 km s<sup>-1</sup>). The observations were made by frequency switching over 20 MHz; in order to increase the sensitivity, the reference channels were later folded with the observation channels, so that an effective velocity range of 52 km s<sup>-1</sup> was covered in each scan. This velocity interval was centered on  $V_{LSR} = +10$  km s<sup>-1</sup>. Each scan was taken with an integration time of 3 minutes. Several peak positions were observed more than once in order to check data quality and system stability. The receiver was calibrated against a room temperature blackbody by a chopper wheel technique in the usual manner.

### b) CO Observations at MWO

The Millimeter Wave Observatory 5 m telescope<sup>1</sup> has a beamwidth (FWHM) of  $2\frac{1}{3}$  and a beam efficiency of 85% at 115 GHz. Most of the observations were made in 1976 April; at that time the receiver had a single-side-band noise temperature varying from 1500 K to 2000 K. The filter-bank had a bandwidth of 10 MHz and a spectral resolution of 250 kHz (corresponding to a velocity resolution of  $0.65 \text{ km s}^{-1}$ ). All observations were made by frequency switching over an interval of 5 MHz, and the data were later folded. Integration time per point was 5 minutes. The area mapped was centered on ON 1 and had dimensions of  $30' \times 35'$ ; several positions around the  $^{12}\text{CO}$  peak were also observed in  $^{13}\text{CO}$  at a frequency of 110 GHz.

In 1979 February we observed an additional ten positions at MWO, not associated with ON 1 itself. Integration time per scan was 3 minutes, and we used the low-noise receiver from the Goddard Institute for Space Studies. The observations were taken with a filter-bank of bandwidth 32 MHz and a channel resolution of 250 kHz. They were frequency-switched and later folded. The temperature scale was corrected for the effects of atmospheric  $\text{O}_2$  absorption using the methods described by Davis and Vanden Bout (1973).

### c) NRAO and OVRO Observations

We used the NRAO and OVRO 10 m dishes to obtain additional high resolution CO profiles in the  $J=1-0$  and  $J=2-1$  transitions. The NRAO<sup>2</sup> observations were made in 1975 with spectral resolutions of 100 and 250 kHz (corresponding to  $0.26$  and  $0.65 \text{ km s}^{-1}$ ), and with integration times of 5 minutes. The temperature scales were corrected following Davis and Vanden Bout (1973). The observations had a spatial resolution of  $70''$  and define a position-velocity map through ON 1.

The OVRO  $^{12}\text{CO}(2-1)$  observations were obtained with the ESTEC/Utrecht receiver and backend, and a spectral resolution of 250 kHz corresponding to a velocity resolution of  $0.325 \text{ km s}^{-1}$ , in a position-switching mode. The spatial resolution was  $26''$ ; details of the instrument and observing procedure can be found elsewhere (F. P. Israel *et al.* 1982, in preparation). Finally, an accurate  $^{12}\text{CO}(1-0)$  profile on ON 1 was obtained with the  $1\frac{1}{7}$  beam of the Bell Labs millimeter telescope in 1982 February.

<sup>1</sup>The Millimeter Wave Observatory (MWO) at Fort Davis, Texas is operated by the Electrical Engineering Research Laboratory, University of Texas at Austin, with support from the National Science Foundation and McDonald Observatory.

<sup>2</sup>The National Radio Astronomy Observatory is operated by Associated Universities, Inc. under contract with the National Science Foundation.

### d) Other Observations

Observations of the  $J_{k_1 k_2} = 2_{12}-1_{11}$  line (140.83953 GHz) of  $\text{H}_2\text{CO}$  were obtained with the  $1\frac{1}{8}$  beam of the MWO telescope using filter-banks of bandwidth 128 and 32 MHz and spectral resolutions of 1 MHz and 250 kHz ( $0.52 \text{ km s}^{-1}$ ). The observations were referenced against a frequency 10 MHz higher than the line frequency. Signal and reference data were then summed appropriately to form a final spectrum, for which the integration time was 1 hour. Observations of the  $J_{k_1 k_2} = 2_{11}-2_{12}$   $\text{H}_2\text{CO}$  line (14.488479 MHz) were made with the  $2'$  beam of the 43 m telescope at the National Radio Astronomy Observatory (NRAO), Green Bank, West Virginia in 1977 November.

The autocorrelator spectrometer was operated at an effective velocity resolution of  $0.26 \text{ km s}^{-1}$  and a total velocity coverage of  $21 \text{ km s}^{-1}$ . The receiver was frequency switched, and a noise tube calibrated the data. The beam efficiency  $\eta_{\text{FSS}} = 0.55$  was taken from Snell (1981) at the elevation appropriate to the observation. Observations of  $\text{HCO}^+$  and a nondetection of  $\text{DCO}^+$  toward ON 1 have already been reported by Wootten, Loren, and Snell (1982); using the same equipment and procedures, we obtained more detailed  $\text{HCO}^+$  observations at NRAO in 1982 June. We also note that both CH and CS have been detected toward ON 1 by other authors (Morris *et al.* 1974; Rydbeck *et al.* 1976), as well as  $\text{NH}_3$  (Ho, Martin, and Barrett 1981).

## III. RESULTS AND ANALYSIS

### a) Molecular Cloud Complexes near ON 1

The results of the low resolution mapping are shown in Figures 1 and 2 and summarized in Table 1. The positions given in Table 1 are those of the center of each cloud, not necessarily the peak position; sizes are estimated from the maps.

As expected, the source ON 1 is associated with a distinct molecular cloud complex. The source does not, however, coincide with the strongest CO emission in the complex. However, the higher resolution MWO observations, which will be discussed in more detail later, show that ON 1 does coincide with a local CO maximum in the cloud complex. The ON 1 CO cloud (cloud 5 in Table 1) is part of a larger complex; in the following we will refer to this complex of CO clouds (clouds 1 through 5 in Table 1) as Cyg MC1 West.

Further mapping has led to the discovery of a second CO cloud complex east of ON 1 that we will refer to as Cyg MC1 East (clouds 8 through 13 in Table 1). Peak intensities in Cyg MC1 East are generally twice as high as in Cyg MC1 West. The overall dimensions of Cyg MC1 West (containing ON 1 itself) are about  $35' \times 80'$ ; those of Cyg MC1 East are about  $50' \times 90'$ .

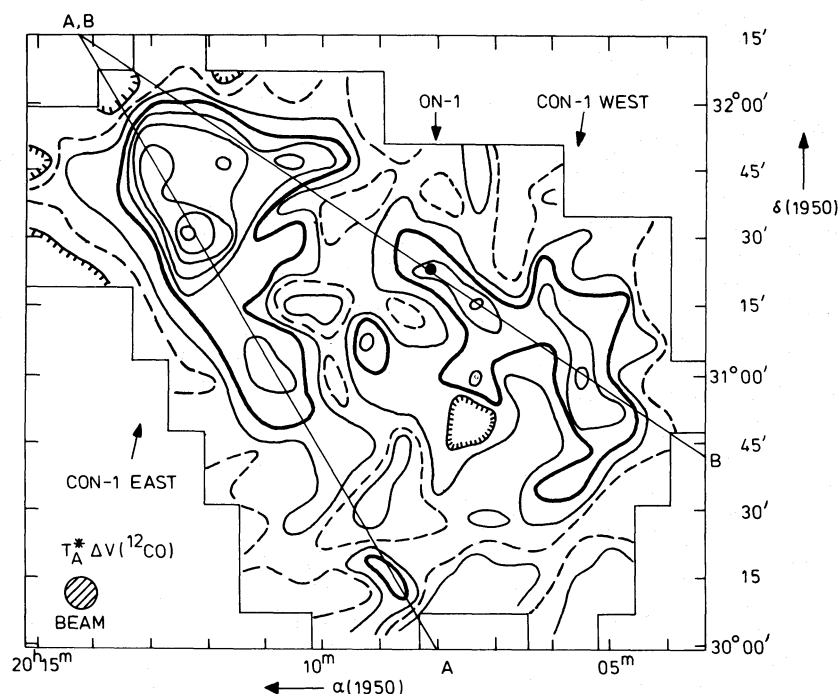


FIG. 1.— $^{12}\text{CO}$  (1–0) map of the ON 1 molecular cloud complex integrated over a velocity range  $V_{\text{LSR}} = -13.5$ – $+36.0$   $\text{km s}^{-1}$ , observed with an 8' beam. The position of ON 1 is marked by a dot. Lines A and B refer to the position-velocity diagrams shown in Fig. 3. Contour values are in steps of  $5.2$   $\text{K km s}^{-1}$ . For the sake of clarity, the  $10.4$   $\text{K km s}^{-1}$  contour is dashed, and the  $20.8$   $\text{K km s}^{-1}$  contour is drawn heavily (CON-1  $\equiv$  Cyg MC-1).

In addition to the velocity information contained in Figure 2 and Table 1, we show position-velocity maps along the lines marked in Figure 1 (Fig. 3). The velocities of the CO peaks in Cyg MC1 West range from  $V_{\text{LSR}} = +8$ – $+12$   $\text{km s}^{-1}$ ; CO velocities in the vicinity of ON 1 itself are around  $V_{\text{LSR}} = +11$   $\text{km s}^{-1}$ . In the Cyg MC1 East complex two distinct subgroups with velocities  $V_{\text{LSR}} = +11$   $\text{km s}^{-1}$  and  $+14$   $\text{km s}^{-1}$  appear to be present. Both CO complexes are elongated and have orientations roughly parallel to the galactic plane, although at some distance from it: about  $\Delta b = -1^\circ 5$  for Cyg MC1 East and  $\Delta b = -1^\circ 0$  for Cyg MC1 West.

Figure 1 shows that CO emission extends south of cloud 6 and south of cloud 2. There is also some emission north of cloud 5.

Since the observed CO emission originates from locations within the solar circle, the observed velocities do not correspond to distances in an unambiguous way. In Table 2 we list near and far distances for some radial velocities at  $l = 69^\circ 5$ .

However, since the CO contours agree very well with the outlines of dark clouds in the Cygnus Rift that are just visible on the red Palomar Sky Survey prints and well visible on the infrared Palomar Sky Survey prints (Hoessel *et al.* 1980)—see Figure 4, it is most probable that the bulk of the observed molecular cloud mass is at the near distance. This leads to the distances quoted in

Table 1, that range from  $D = 0.9$  to  $D = 2.2$  kpc, with ON 1 itself at  $D = 1.4$  kpc. As we will show in the next section, the parameters of the compact CO cloud associated with ON 1 itself also suggest adoption of the near distance to this source.

We should note, however, that actual distances are still somewhat uncertain due to the low velocity of the complex. If, for instance, random velocities of  $2$   $\text{km s}^{-1}$  are present, an uncertainty of about  $0.5$  kpc (cf. Table 2) is introduced, corresponding to an error of about 30% in the values listed in Table 1.

The area occupied by the two CO complexes is only partly covered by the Maryland-Green Bank H I survey (Westerhout 1969). In the (western) part covered, no clear relation between H I and CO emission features is found, although most of the CO emission is seen at positions close to a weak H I feature at  $V_{\text{LSR}} = +14$   $\text{km s}^{-1}$  located on the flank of a strong H I ridge at  $V_{\text{LSR}} = +7$   $\text{km s}^{-1}$  (corresponding to distances of 1 and 6 kpc).

Summarizing this section, we conclude that ON 1 is associated with one of two previously unknown large molecular cloud complexes. These molecular cloud complexes are visible as dark clouds on Palomar Sky Survey prints. They are located at a distance of about 1.4 kpc, and their dimensions are  $15 \times 35$  pc and  $20 \times 40$  pc, respectively. The western complex associated with ON 1

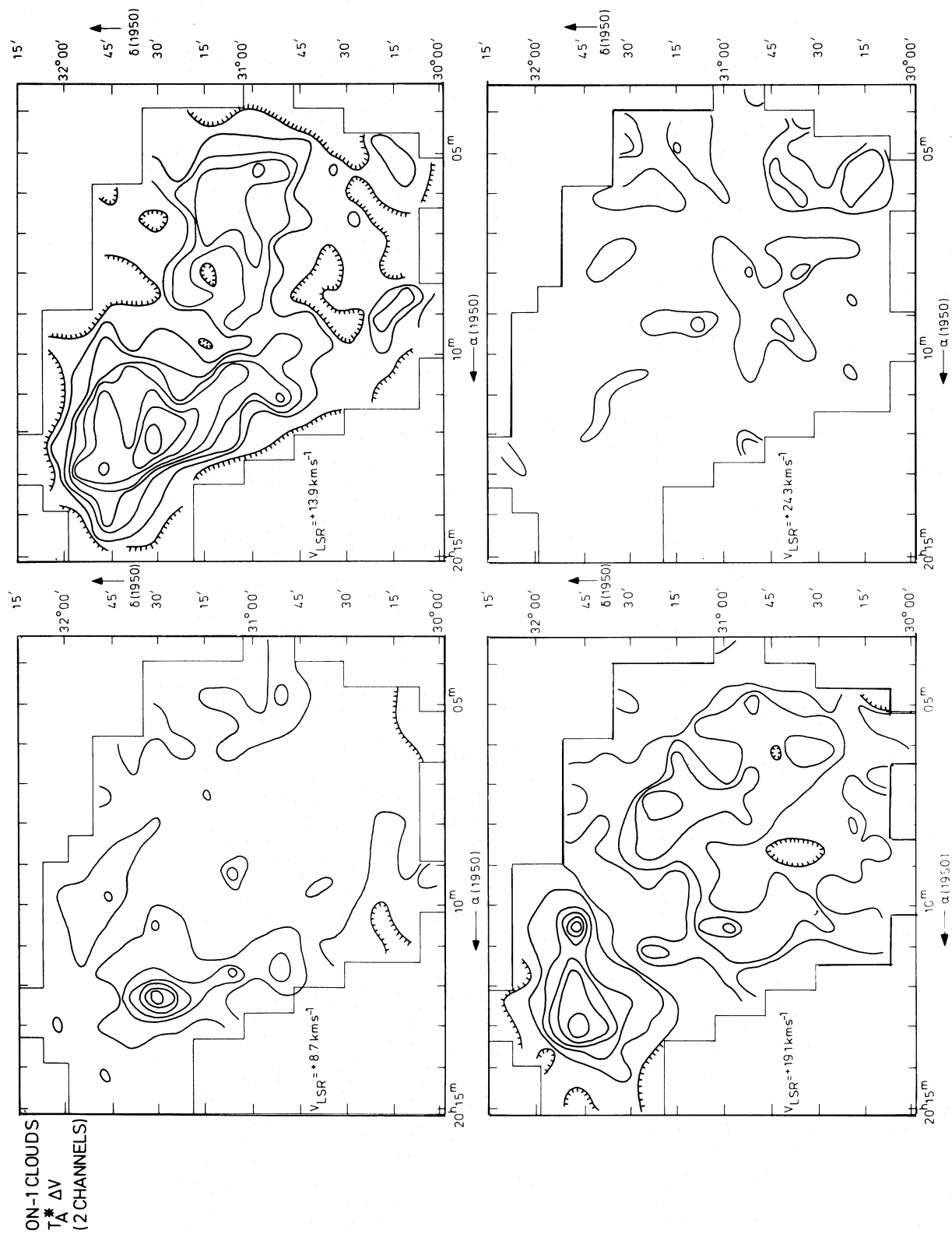


FIG. 2.— $^{12}\text{CO}(1-0)$  maps of the ON 1 molecular cloud complex integrated over two velocity channels ( $5.2 \text{ km s}^{-1}$ ) each. Contour values are in steps of  $2.6 \text{ K km s}^{-1}$ .

TABLE 1  
CO CLOUDS NEAR ON 1 (WITH 8' RESOLUTION)

Name <sup>a</sup>	$\alpha(1950)$	$\delta(1950)$	$T_A^*$ (peak) (K)	$V_{\text{LSR}}$ ( $\text{km s}^{-1}$ )	$\Delta V$ ( $\text{km s}^{-1}$ )	Angular Size (arcmin)	$D$ (kpc)	Linear Size (pc) <sup>b</sup>
1 .....	20 <sup>h</sup> 05 <sup>m</sup> 5 <sup>s</sup>	+31°00'	2.8	12.2	8.3	12×32	1.6	5.7×15.2
2 .....	20 05.8	30 35	1.7	8.0	15.6	8×12	0.9	2.1×3.1
3 .....	20 07.3	30 27	1.1	7.9	14.6	~ 8	0.9	~ 2.1
4 .....	20 07.4	31 00	3.1	12.1	6.2	~ 12	1.6	~ 5.6
5 .....	20 07.4	31 13	2.8	11.0	6.5	8×25	1.4	3.3×10.2
ON 1 <sup>c</sup> .....	20 08.2	31 23	2.8	11.0	5.6	...	1.4	...
6 .....	20 08.6	30 13	2.4	12.6	5.0	8×12	1.7	3.9×5.9
7 .....	20 09.2	31 07	2.3	13.9	12.5	~ 12	2.1	~ 7.3
8 .....	20 10.5	31 48	3.5	10.9	5.2	8×15	1.4	3.3×6.1
9 .....	20 10.5	31 32	2.2	13.5	6.2	~ 10	1.9	~ 5.5
10 .....	20 11.1	31 05	3.6	14.7	4.2	20×12	2.2	12.8×7.7
11 .....	20 11.8	31 48	4.7	10.7	6.2	~ 8	1.4	~ 2.3
12 .....	20 12.4	31 31	5.2	14.3	8.3	~ 15	2.1	~ 9.1
13 .....	20 12.9	31 45	5.0	11.2	6.8	~ 10	1.4	~ 4.1

<sup>a</sup>Cyg MC1 West consists of clouds 1, 2, 3, 4, and 5; Cyg MC1 East consists of clouds 8, 9, 10, 11, 12, and 13.  
<sup>b</sup>Linear diameter is based on near distance—see text.  
<sup>c</sup>Part of cloud 5.

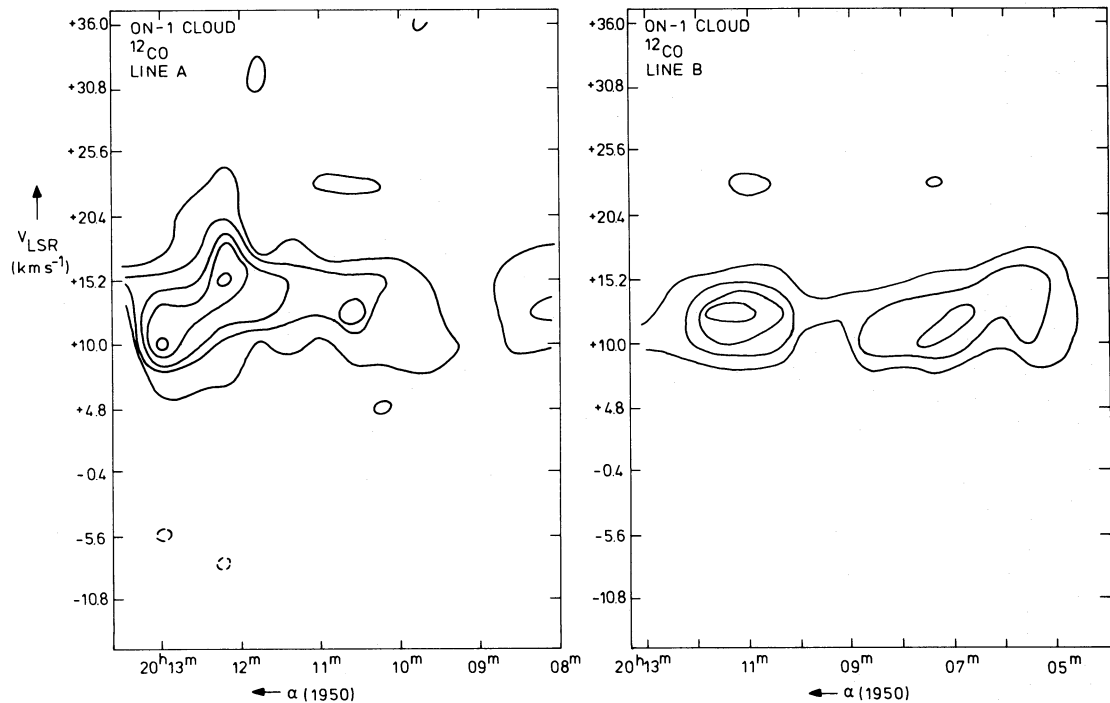


FIG. 3.—Position-velocity diagrams along lines A and B in Fig. 1



TABLE 2  
VELOCITY-DISTANCE RELATION AT  $l = 69^\circ 5$

$V_{\text{LSR}}$ (km s $^{-1}$ )	Near Distance (kpc)	Far Distance (kpc)
+ 5 .....	0.6	6.4
+ 10 .....	1.2	5.8
+ 15 .....	2.3	4.8
+ 18.7 .....	3.5	3.5

itself has typical peak CO line strengths  $T_A^* \Delta V = 20$  K km s $^{-1}$  in the 8' Columbia beam; the corresponding value for the eastern complex is  $T_A^* \Delta V = 30$  K km s $^{-1}$ .

b) *The CO Cloud Associated with ON 1*

Figures 5 and 6 show the mapping results obtained with the MWO 5 m telescope at a resolution of 2.3, which is 3.5 times better than the resolution of the data described in the previous section. The area mapped is  $28'' \times 35''$  and contains four major and three minor peaks, all part of cloud 5 from Table 1; an extension in the direction of cloud 4 is also visible in Figure 5. The characteristics of the CO maxima are given in Table 3. Although ON 1 is located near the position of peak antenna temperature, a 10% higher  $T_A^*$  is measured one beamwidth SWW of the object. ON 1 does coincide, however, with the peak in the integrated  $^{12}\text{CO}$  emission, as well as with the peak in both the  $^{13}\text{CO}$  antenna temperature and column density maps.

We have calculated column densities  $N(^{13}\text{CO})$  under the usual LTE associations; the result is also shown in Figure 5. This shows a cloud with dimensions of  $5.6 \times 2.9$ , corresponding to  $2.0 \times 0.7$  pc after (gaussian) deconvolution of the beam profile. The orientation of the source is SE-NW, roughly at right angles to the major axis of cloud 5 from Table 1. The  $N(^{13}\text{CO})$  map shows a great similarity to the  $T_A^* \Delta V(^{12}\text{CO})$  map and suggests a structure that can best be described as a bright core embedded in a more diffuse envelope.

i) *The Envelope Component of the ON 1 Cloud*

The envelope component is well resolved and clearly shown in Figures 5 and 6. Its  $^{12}\text{CO}$  size is about 12' (or 5 pc). It is relatively sharply delineated in the east, where the integrated emission drops quickly to about 15% of the peak intensity. This is also seen in Figure 7, which shows position velocity diagrams along lines marked in Figure 5a. Along line A, the median velocity is roughly constant at  $V_{\text{LSR}} = +11$  km s $^{-1}$ ; Line B follows the major axis of the ON 1 CO cloud as seen in Figure 5d; it shows a velocity shift of about 3 km s $^{-1}$  over a distance of 25' (10 pc). In Figure 7 the strong increase in  $^{12}\text{CO}$  linewidth from about 2 km s $^{-1}$  to 6 km s $^{-1}$  at the position of ON 1 is easily seen, as well as

the slight increase in  $^{12}\text{CO}$  peak antenna temperature towards the SSW, which was mentioned before.

The region immediately outside the core has a relatively low  $^{13}\text{CO}$  column density of order  $N(^{13}\text{CO}) = 10^{15}$  cm $^{-2}$ . Assuming  $N(\text{H}_2)/N(^{13}\text{CO}) = 5 \times 10^5$  (Dickman 1978), we estimate an envelope of  $M(\text{H}_2) = 200 M_\odot$  with a mean density of about  $n(\text{H}_2) = 15$  cm $^{-3}$ .

ii) *The Core Component of the ON 1 Cloud*

The coincidence of ON 1 with the peak in the  $^{13}\text{CO}$  map shows that the compact H II region/maser source is located in the densest part of the cloud. Integration of the  $N(^{13}\text{CO})$  contours in Figure 5d yields a total core mass of  $M(\text{H}_2) = 560 M_\odot$  [again assuming  $N(\text{H}_2)/N(^{13}\text{CO}) = 5 \times 10^5$ ] and a mean density  $n(\text{H}_2) = 2350$  cm $^{-3}$ , assuming a source depth of 1.2 pc, equal to the mean diameter of the  $^{13}\text{CO}$  core. These values are typical for a compact, star-forming molecular cloud core.  $\text{NH}_3$  observations by Ho, Martin, and Barrett (1981) yield a mean density  $n(\text{H}_2) \approx 2100$  cm $^{-3}$  (after correction to  $D = 1.4$  kpc), in very good agreement with our result. The  $\text{NH}_3$  peak coincides with ON 1 itself. Adoption of the far distance of 5.6 kpc, on the other hand, would yield a molecular mass 16 times higher, a space density 4 times smaller, and a linear size 4 times larger. Though not impossible, these parameters are nevertheless less plausible for such a cloud core.

At the position of the H II region and the line broadening, emission from the  $\text{HCO}^+$  and  $\text{H}_2\text{CO}$  molecules occurs, confirming the presence of very high densities. Our observations of  $\text{HCO}^+$  are shown in Figure 8, and those of  $\text{H}_2\text{CO}$  are shown in Table 4 and in Figure 9.

In principle, the  $\text{H}_2\text{CO}$  observations may also be used to infer the mean density of the core. Unfortunately, the precise location of the continuum source relative to the molecular material is unknown. This source is, however, so weak at 2 cm that most of the 2 cm absorption must be against the cosmic background radiation. Assuming no continuum contribution and utilizing a large velocity gradient model (Wootten, Snell, and Evans 1980) we estimate the density to be  $N(\text{H}_2) \geq 10^4$  cm $^{-3}$ . The formaldehyde abundance required to reproduce the 2 mm and 2 cm lines is  $X(\text{H}_2\text{CO}) \approx 10^{-9}$ , similar to the abundances found in the survey of Wootten, Snell, and Evans (1980). None of the cold clouds in that survey showed evidence of star formation. In this respect ON 1 is unusual. Combining our results with the CH results by Rydbeck *et al.* (1976) we find  $N(\text{CH})/N(\text{CO}) \approx 1.5 \times 10^{-3}$  (assuming  $[^{12}\text{CO}]/[^{13}\text{CO}] = 69$ ), again much closer to what is expected for cold clouds than for clouds associated with star formation (cf. Table 8, Rydbeck *et al.* 1976).

Recently, Forster, Goss, and Dickel (1982) obtained aperture synthesis observations of the 6 cm  $\text{H}_2\text{CO}$  absorption against ON 1. They find two absorption peaks



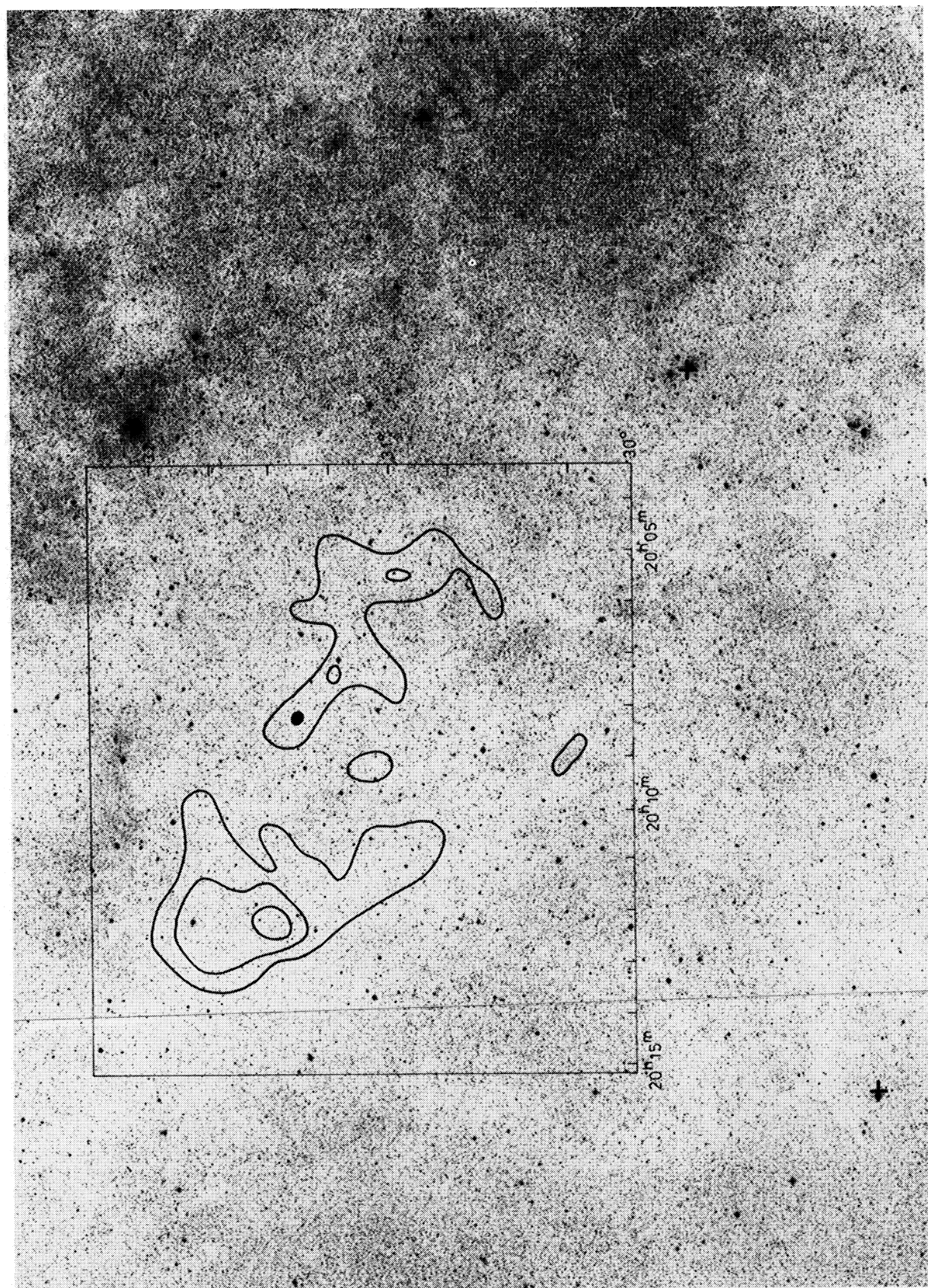


FIG. 4.—Overlay of the molecular cloud outlines from Fig. 1 on the red Palomar Sky Survey print. The position of ON 1 is marked by a dot.



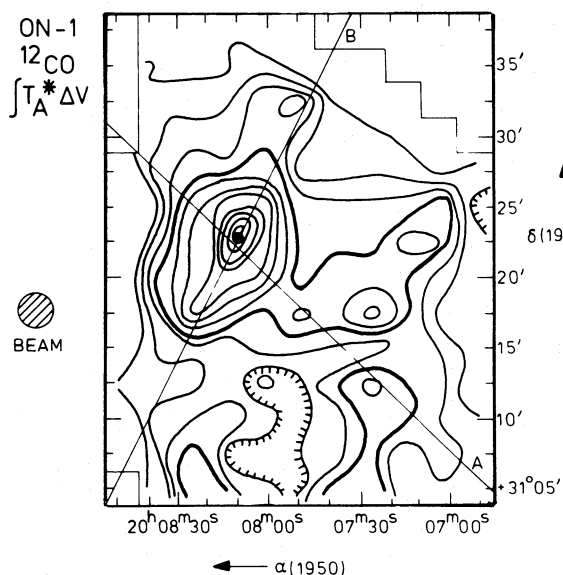


FIG. 5a

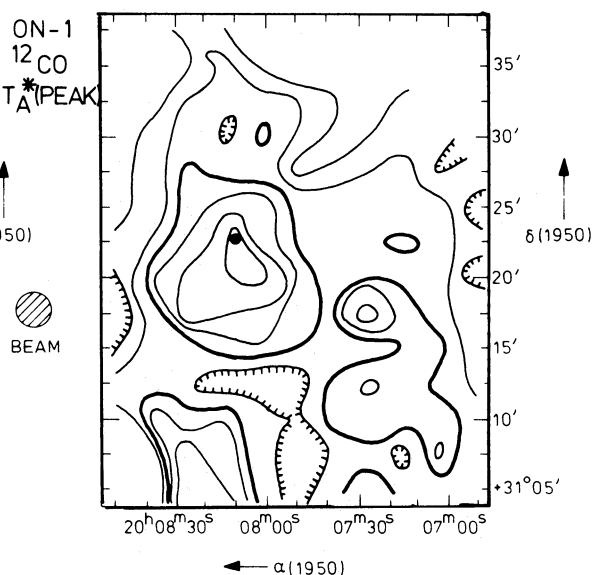


FIG. 5b

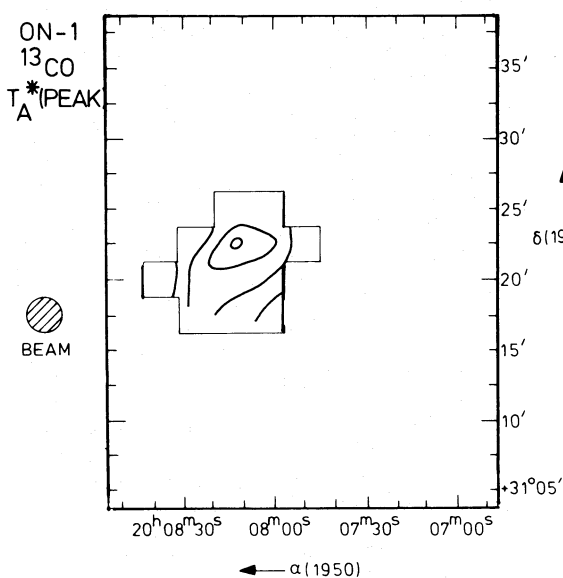


FIG. 5c

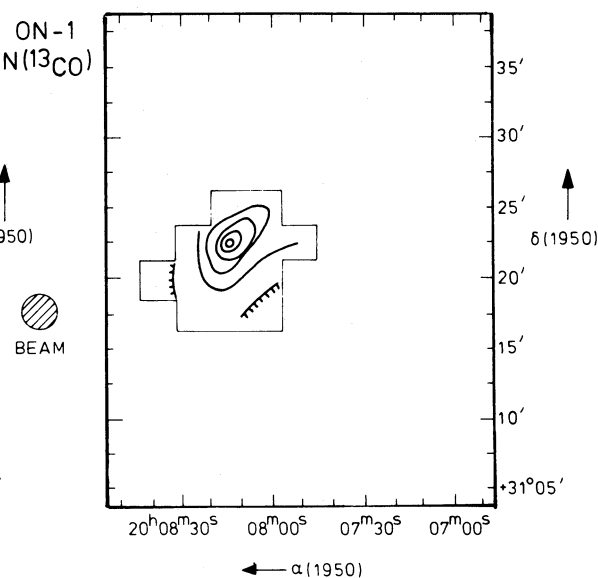


FIG. 5d

FIG. 5.—CO(1-0) maps of the ON 1 molecular cloud and its immediate vicinity observed with a 2/3 beam. (a)  $^{12}\text{CO}$  map integrated over a velocity range  $V_{\text{LSR}} = +4.0 - +16.0 \text{ km s}^{-1}$ . The position of ON 1 is marked by a dot. Lines A and B refer to the position-velocity diagrams in Fig. 7. Contours are in steps of  $3.25 \text{ K km s}^{-1}$ ; lowest contour is  $6.5 \text{ K km s}^{-1}$ . For the sake of clarity, the  $16.25 \text{ K km s}^{-1}$  contour is drawn heavily. (b)  $^{12}\text{CO}$  peak antenna temperature map. Contours are in steps of  $1 \text{ K}$ ; lowest contour is  $2 \text{ K}$ . For the sake of clarity, the  $4 \text{ K}$  contour is drawn heavily. (c)  $^{13}\text{CO}$  peak antenna temperature map. Contours are in steps of  $1 \text{ K}$ . (d) Map of column density  $N(^{13}\text{CO})$ . Contours are in steps of  $3 \times 10^{15} \text{ cm}^{-2}$ .



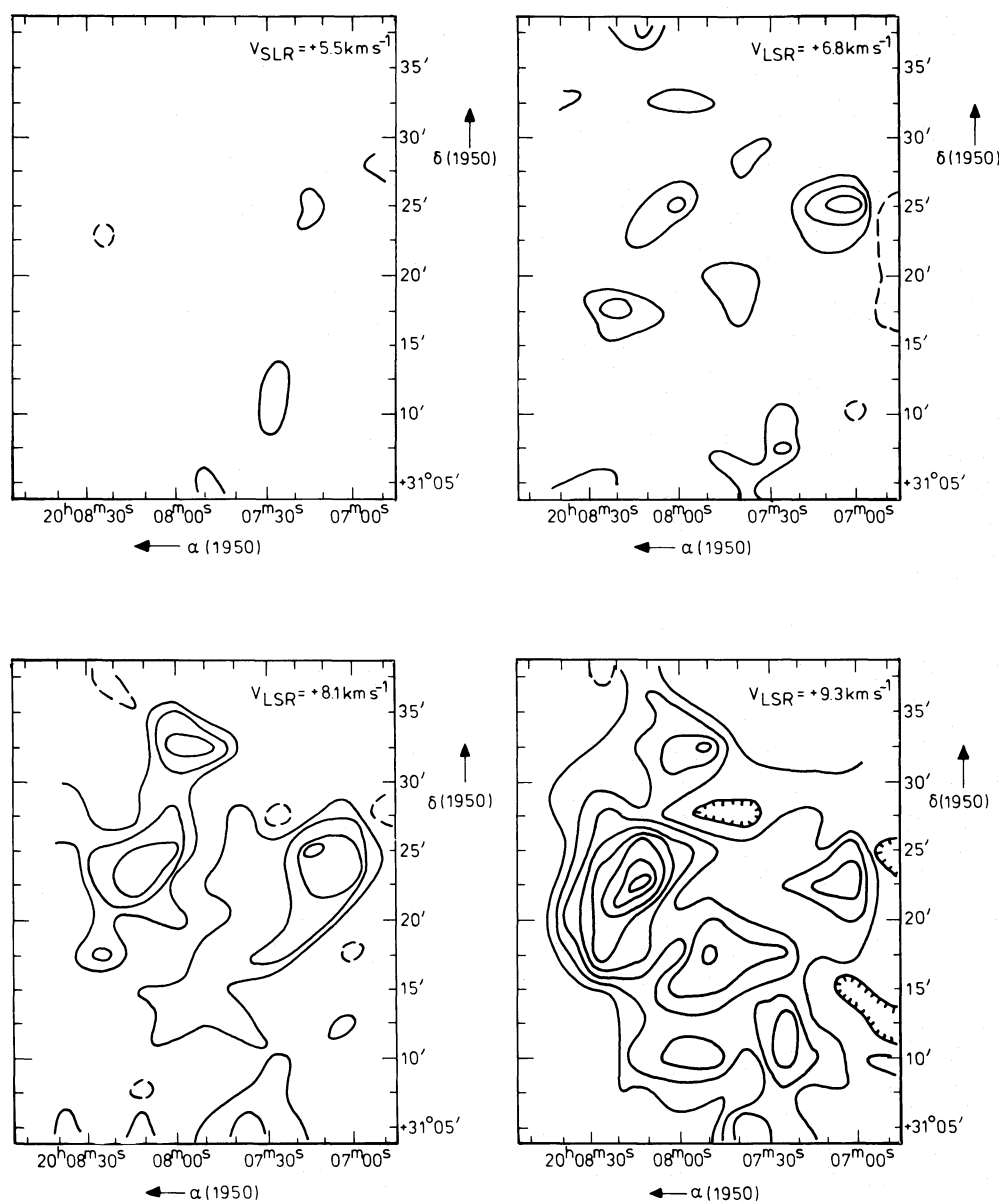


FIG. 6.— $^{12}\text{CO}(1-0)$  maps of the ON 1 molecular cloud integrated over two velocity channels ( $1.3 \text{ km s}^{-1}$ ) each. Contours are in steps of  $1 \text{ K km s}^{-1}$ . Maps containing only noise are not shown.

at  $V_{\text{LSR}} = +8$  and  $+11 \text{ km s}^{-1}$ , both with optical depths  $\tau \sim 2$ . From their observations, again very high molecular densities  $n(\text{H}_2) \geq 10^5$  and probably much higher can be derived, in very good agreement with the above estimates.

Concomitant with the apparent high density of the ON 1 molecular cloud core, there is strong evidence for self-absorption in this core. The coincidence of ON 1 with the position of strong line-broadening shows that it is the center of activity in the cloud. The increase in line width is seen particularly clear in Figure 10, which is a declination-velocity map through the core component

made with the  $70''$  beam of the NRAO millimeter telescope. The peak intensity in the line tends to shift to higher velocities, developing a broad low velocity wing in the process. This by itself already suggests absorption by low excitation CO lying along the line of sight. The suggestion is strengthened by a comparison of the high resolution  $^{12}\text{CO}$  observations in the  $J=2-1$  and  $J=1-0$  transitions summarized in Table 5. The above argument is strengthened considerably by the new  $\text{HCO}^+$  observations. The  $\text{HCO}^+$  map (Fig. 8) shows that the extent of the dense core is roughly  $2''$ , or  $0.8 \text{ pc}$  at a distance of  $1.4 \text{ kpc}$ . This size is comparable to the  $1.5$  ( $0.6 \text{ pc}$ ) core

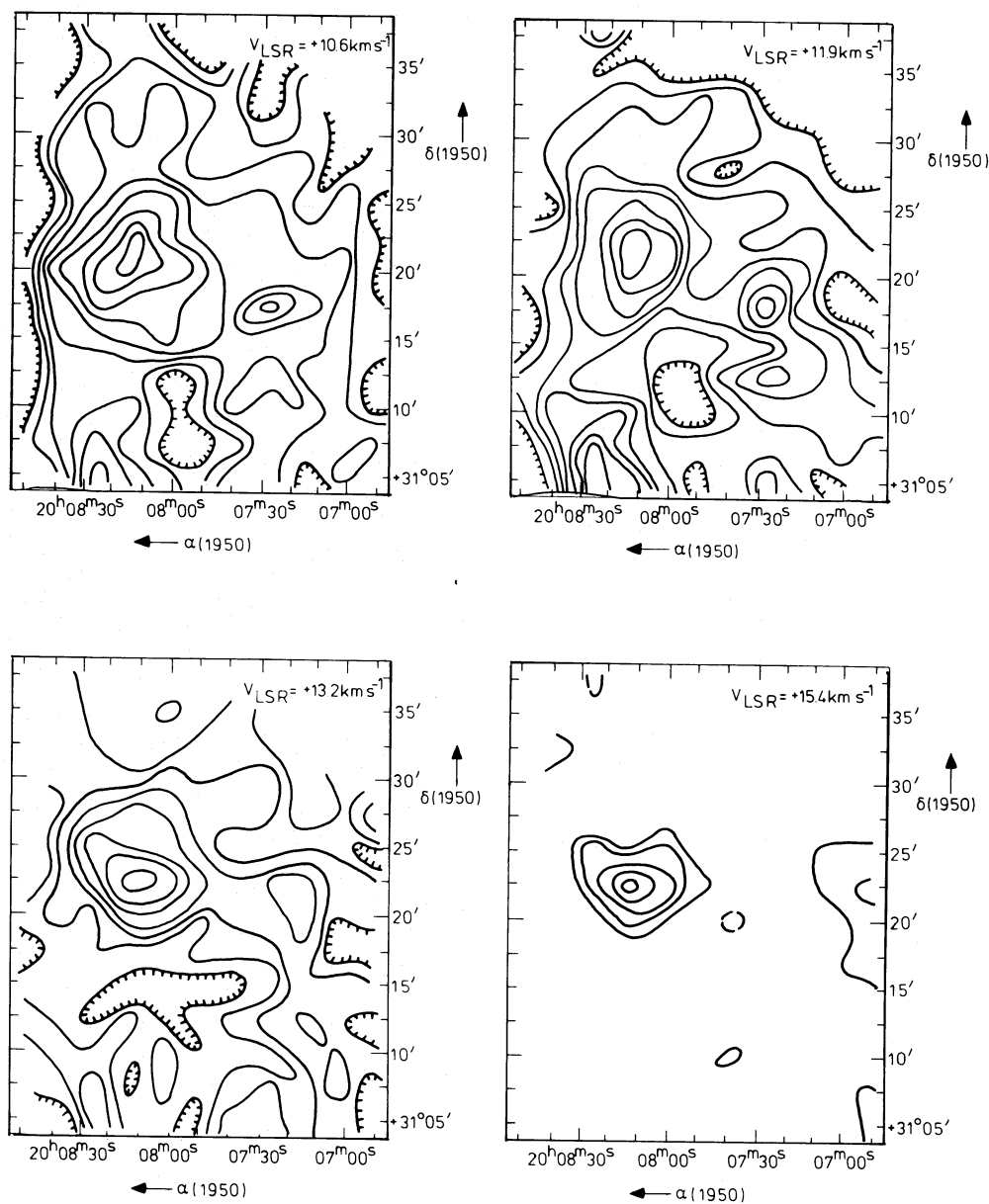


FIG. 6.—Continued

radius found by Ho, Martin, and Barrett (1981) from  $\text{NH}_3$  observations. The core extent is also comparable to the mean  $\text{HCO}^+$  core radius of 0.6 pc found by Wootten, Snell, and Evans (1980) in a sample of star forming clouds.

Although the  $\text{NH}_3$  and  $\text{H}_2\text{CO}$  lines center about  $V_{\text{LSR}} = +11.4 \text{ km s}^{-1}$ , the  $\text{HCO}^+$  lines peak at velocities of  $+9$  and  $+14 \text{ km s}^{-1}$  near the core. At these positions, the profiles feature a minimum temperature near  $+11 \text{ km s}^{-1}$ . This local minimum undoubtedly results from absorption by foreground material of low excitation temperature. In many star forming clouds,  $\text{HCO}^+$

profiles resemble those of CO, showing both self-absorption and broad line wings near embedded infrared objects (Loren and Wootten 1980). The profiles of  $\text{HCO}^+$  and CO in the ON 1 core follow this trend. In fact, if the core temperature were as low as the 10 K suggested by the CO profile, deuteration of  $\text{HCO}^+$  might proceed to the high levels typical of cold dark clouds (Wootten, Loren, and Snell 1982). Limits to  $\text{DCO}^+ J=2-1$  emission, reported by Wootten, Loren, and Snell (1982), and to the  $J=1-0$  emission of  $T_A^* < 0.4 \text{ K}$  ( $2\sigma$ ), which we have measured, are consistent with a warmer temperature for the core. Confirming this con-

TABLE 3  
CO CLOUDS NEAR ON 1 (WITH 2/3 RESOLUTION)

Name	$\alpha(1950)$	$\delta(1950)$	$T_A^*$ (peak) (K)	$V_{\text{LSR}}$ ( $\text{km s}^{-1}$ )	$\Delta V$ ( $\text{km s}^{-1}$ )	Size (arcmin)
1.....	20 <sup>h</sup> 07 <sup>m</sup> 03 <sup>s</sup> .5	+31°07'5	5.0	12.0	3.1	≤ 2.5
2.....	20 07 12.3	31 22.5	3.6	+10.3	6.5	4×2.5
3.....	20 07 25.8	31 12.3	5.0	+11.0	4.4	~ 3
4.....	20 07 25.8	31 17.5	6.8	+10.6	4.7	~ 3
5.....	20 07 48.8	31 17.5	4.7	+10.6	4.8	≤ 2.5
6.....	20 07 52.3	31 32.2	3.5	+9.7	5.2	~ 3
7 (ON 1) ...	20 08 10.0	31 22.7	7.1	+11.3	6.2	7×12

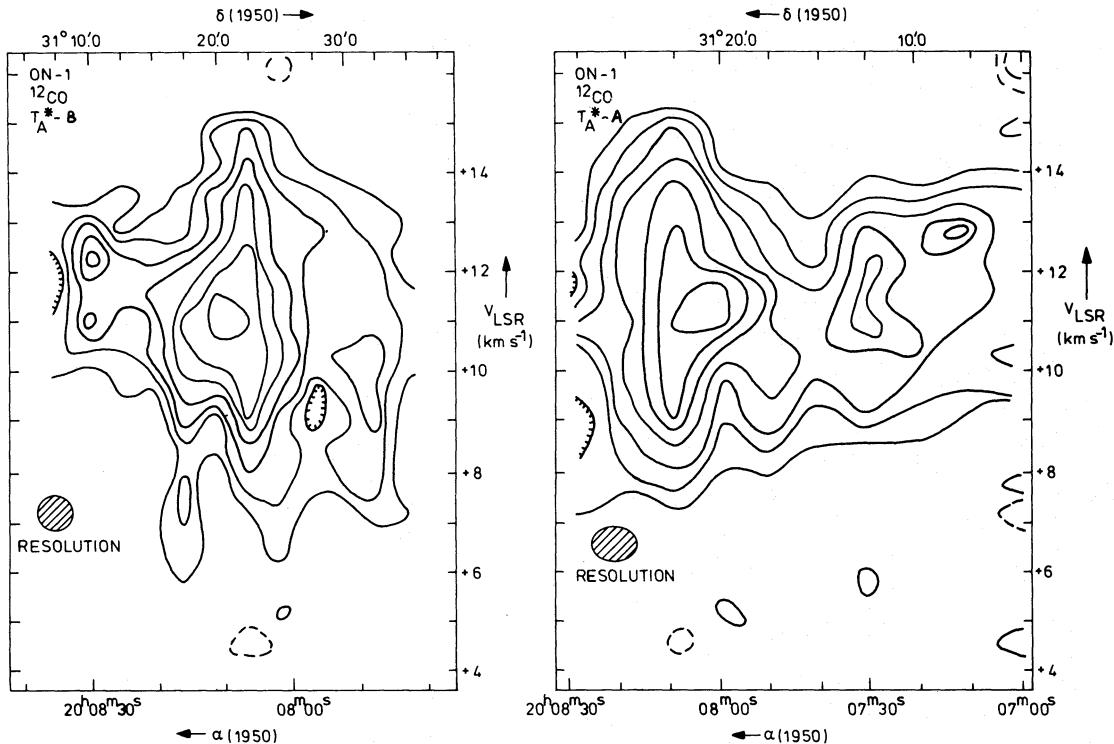


FIG. 7.—Position-velocity maps along lines A and B in Fig. 5a. Contours are in steps of 1 K

jecture, warm dust in the core has been observed by Sargent *et al.* (1981) who derive a lower limit to the dust temperature of 35 K from their infrared observations. We conclude that a substantial region of cool, moderately dense material lies between us and the star forming core of ON 1, which is substantially warmer than indicated by the intensity of the CO line.

Turning back again to the  $\text{HCO}^+$  map (Fig. 8) there are even hints of a redshift/blueshift asymmetry, in the sense that the dominant  $\text{HCO}^+$  wings are redshifted from the central velocity west and south of ON 1, and blueshifted east and south of ON 1. In addition the central  $\text{HCO}^+$  profile may exhibit a weak plateau-like feature over a range of about  $30 \text{ km s}^{-1}$ , whereas the

Bell Labs 1/7 central  $^{12}\text{CO}$  profile likewise shows indication for the presence of a plateau with  $T_A^*$  (peak)  $\approx 0.5 \text{ K}$ , and a range of again  $30 \text{ km s}^{-1}$ . Thus, in addition to strong self-absorption, ON 1 also seems to show characteristics usually associated with bipolar mass-outflow phenomena (see, e.g., Bally and Lada 1983).

Thus we picture ON 1 as a center of star forming activity located within a dense cool core. While IRS 1 (Lunel *et al.* 1980) may be associated with this region, IRS 2 (lying 3' south) for two reasons, probably is not. Lunel *et al.* cite positional coincidence of IRS 2 with a CO peak as evidence for its association with the cloud. As we have seen, self-absorption weakens the CO line in the core, resulting in underestimate of the core tempera-



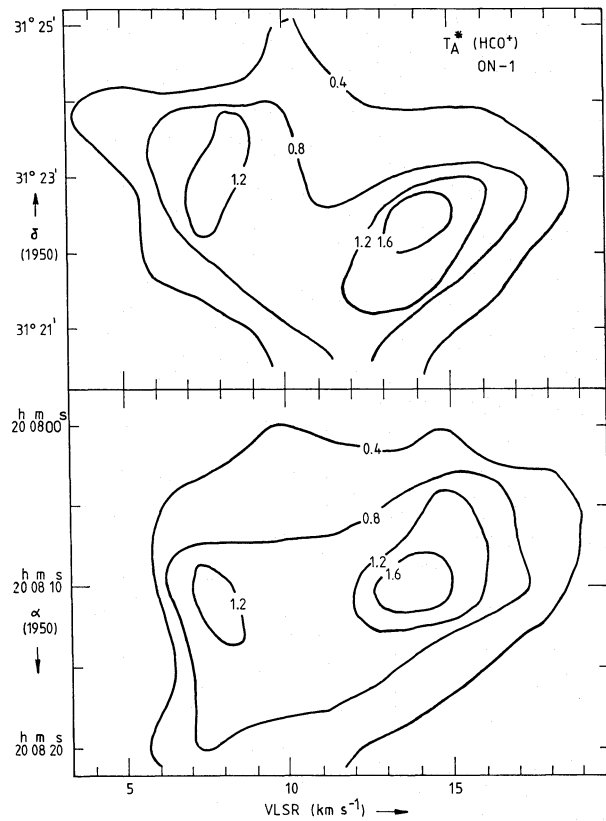


FIG. 8.—Position-velocity maps of intensity of the  $J=1-0$   $\text{HCO}^+$  line toward the core of ON 1 as observed with the NRAO antenna. Velocity resolution is  $0.84 \text{ km s}^{-1}$ , and contours are drawn at the  $2.5 \sigma$  level. The apparent existence of two peaks in this line results from superposition upon the core of an absorbing lane of cold foreground material located in front of the core. The upper panel shows a path through the core in declination, the lower in right ascension.

ture. Away from the core, self-absorption is less strong, and the peaking of CO which occurs to the south is probably only a “virtual” peak, not associated with an actual temperature enhancement in the cloud. Association of IRS 2 with the cloud is not necessary to explain temperature enhancement. Furthermore, IRS 2 lies outside the dense core of the cloud.

### c) CO Observations of Other Clouds

To investigate the nature of the  $^{12}\text{CO}$  peaks in clouds 7 and 12 (Table 1) limited maps were made with the MWO 2/3 beam. Some representative profiles are shown in Figure 11. Cloud 7 is the small, seemingly isolated cloud  $25'$  SE of ON 1. Its CO intensities of  $T_A^* = 3-5 \text{ K}$  are comparable to those of the other CO clouds near ON 1 (Table 3), and the line widths of about  $3 \text{ km s}^{-1}$  do not indicate the presence of centers of star forming activity. From the limited data available we infer that the intensity maximum is located near  $\alpha(1950) = 20^{\text{h}}09^{\text{m}}07^{\text{s}}$ ,  $\delta(1950) = +31^{\circ}06'0$ .

Cloud 12 is the brightest peak in the Cyg MC1 East complex (cf. Fig. 1). Its maximum temperature occurs near  $\alpha(1950) = 20^{\text{h}}11^{\text{m}}53^{\text{s}}$ ,  $\delta(1950) = +31^{\circ}27'5''$ . With  $T_A^* = 11 \text{ K}$ , it is significantly brighter than the ON 1 CO peak ( $T_A^* = 7 \text{ K}$ ), observed with the same beam. Over most of the area, two velocity components are observed at  $V_{\text{LSR}} = +15 \text{ km s}^{-1}$  (main peak) and  $V_{\text{LSR}} = +6 \text{ km s}^{-1}$ . Traces of the latter component are visible in the lower resolution position-velocity map (Fig. 3). The profiles in Figure 11 also show a lower intensity, higher velocity wing at  $V_{\text{LSR}} = +18-+20 \text{ km s}^{-1}$  that can likewise be recognized in Figure 4 and may arise from a spatially separate component (cf. Table 2).

The complex line spectra and the relatively high CO intensity of cloud 12 make it an interesting candidate for further study. Preliminary WSRT aperture synthesis radio continuum observations at  $0.6 \text{ GHz}$  fail to show

TABLE 4  
MOLECULAR LINES IN THE CORE OF ON 1

Line	Transition	Frequency (GHz)	$T_R$ (K)	$V_{\text{LSR}}$ ( $\text{km s}^{-1}$ )	$\Delta V$ ( $\text{km s}^{-1}$ )
$^{12}\text{CO}$ ....	$1 \rightarrow 0^a$	115.271	$10.0 \pm 0.3$	$+9.5$ }	7.5
	$1 \rightarrow 0^a$	115.271	$8.0 \pm 0.3$	$+13.5$ }	
$\text{HCO}^+$ ...	$1 \rightarrow 0$	89.189	$1.4 \pm 0.2$	$+8.5$ }	7.0
	$1 \rightarrow 0$	89.189	$2.0 \pm 0.2$	$+13.5$ }	
$\text{DCO}^+$ ...	$1 \rightarrow 0$	72.039	$< 0.4$	...	...
	$2 \rightarrow 1^b$	144.077	$< 0.15$	...	...
$\text{H}_2\text{CO}$ ....	$2_{12} \rightarrow 1_{11}$	140.840	$0.6 \pm 0.2$	10.8	7.0
	$2_{11} \rightarrow 2_{12}$	14.488	$-0.4 \pm 0.1$	11.1	2.4
	$2_{11} \rightarrow 2_{12}$	14.488	$-0.1 \pm 0.1^c$	11.2	3.1

<sup>a</sup>Obtained with  $1.7'$  beam at Bell Labs.  
<sup>b</sup>From Wootten, Loren, and Snell 1982.  
<sup>c</sup> $2'$  south of ON 1.

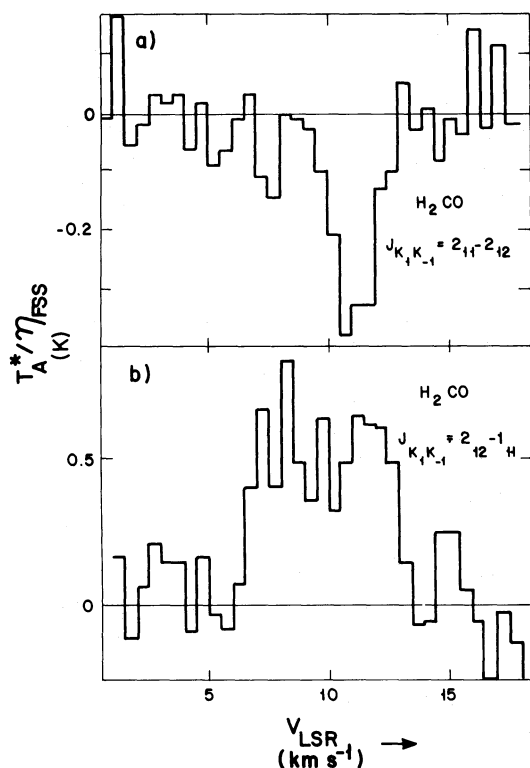


FIG. 9.—H<sub>2</sub>CO observations on ON 1. (a) Absorption profile at  $\lambda = 2$  cm. (b) Emission profile at  $\lambda = 2$  mm.

any emission near this cloud, but further molecular line and radio continuum observations at higher resolutions and sensitivities are in progress.

#### IV. DISCUSSION

The ON 1 source complex shows all classical signposts of star formation; that is, it shows all phenomena commonly associated with the interaction between a newly formed OB star and the surrounding dense interstellar medium. The H<sub>2</sub>O maser emission associated with ON 1 originates in two clusters with sizes of 0.005 and 0.001 pc, and separated by 0.016 pc (Downes *et al.* 1979, corrected to a distance of 1.4 kpc). The largest of the two clusters coincides with the OH maser (Hardebeck 1972) and with the compact H II region. This compact H II region has a size of about 1'' or 0.007 pc; it is completely isolated in the sense that no other H II region has been found within several parsecs (Harris 1974; Matthews *et al.* 1977; J. Turner and B. Baud 1981, private communication).

Recently, Becklin, Downes, Genzel, and Wynn-Williams obtained a 20  $\mu$ m mid-infrared map of the ON 1 source complex with the IRTF (R. Genzel 1981, private communication). This is the only continuum map that shows structure: two maxima are seen with a separation of 9'' (0.060 pc). Within the error bars, the minor northern infrared maximum coincides with the H II region/OH maser/H<sub>2</sub>O maser complex. The nature of the southern infrared maximum is at this moment uncertain. Both the optically thin radio flux density

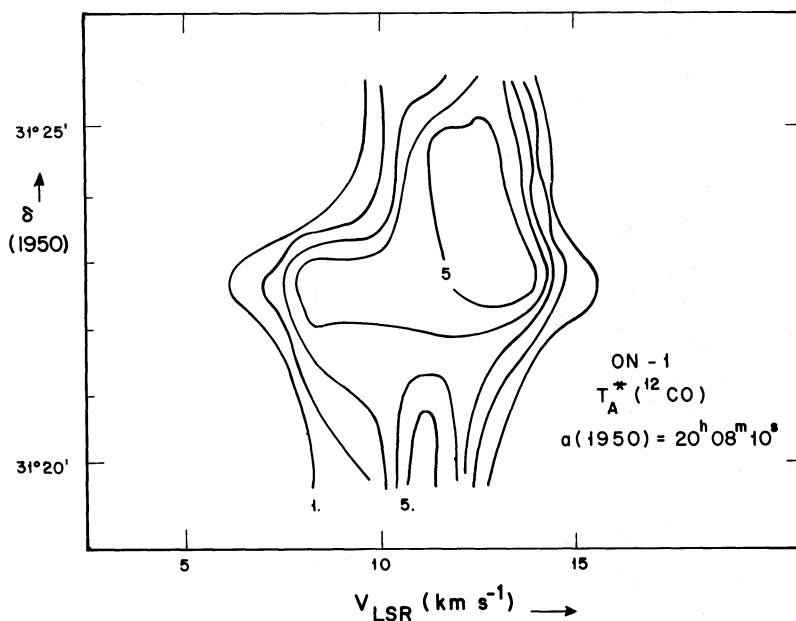


FIG. 10.—<sup>12</sup>CO(1-0) declination-velocity map through ON 1, observed with a 1.1 beam. Contour values are in steps of 1.5 K (corrected for telescope beam efficiency  $\eta_{\text{fss}} = 0.65$ ).

TABLE 5  
COMPARISON OF  $^{12}\text{CO}$  OBSERVATIONS OF ON 1  
WITH DIFFERENT BEAMWIDTHS

Position	Observatory	Line Transition	HPBW (arcmin)	Velocity Resolution ( $\text{km s}^{-1}$ )	$T_A^*$ (K)	$\Delta V$ ( $\text{km s}^{-1}$ )
(0,0) .....	Columbia	$1 \rightarrow 0$	8	2.6	2.8	6.5
	MWO	$1 \rightarrow 0$	2.3	0.65	7.1	6.2
	Bell Labs	$1 \rightarrow 0$	1.7	0.65	10.0	7.5
(0,0) .....	OVRO	$1 \rightarrow 0$	1.0	0.51	13.0	9.0
	OVRO	$2 \rightarrow 1$	0.5	0.33	11.2	8.0
	OVRO	$2 \rightarrow 1$	0.1	0.65	10.5	8.0
(-1,0) ....	OVRO	$1 \rightarrow 0$	1.0	0.51	8.1	7.0
	OVRO	$2 \rightarrow 1$	0.5	0.33	11.3	4.0
(+1,0) ....	OVRO	$1 \rightarrow 0$	1.0	0.51	12.0	6.5
	OVRO	$2 \rightarrow 1$	0.5	0.33	14.6	4.0
(0,+1) ....	OVRO	$2 \rightarrow 1$	0.5	0.33	13.3	4.5
(0,-1) ....	OVRO	$2 \rightarrow 1$	0.5	0.33	8.9	4.0

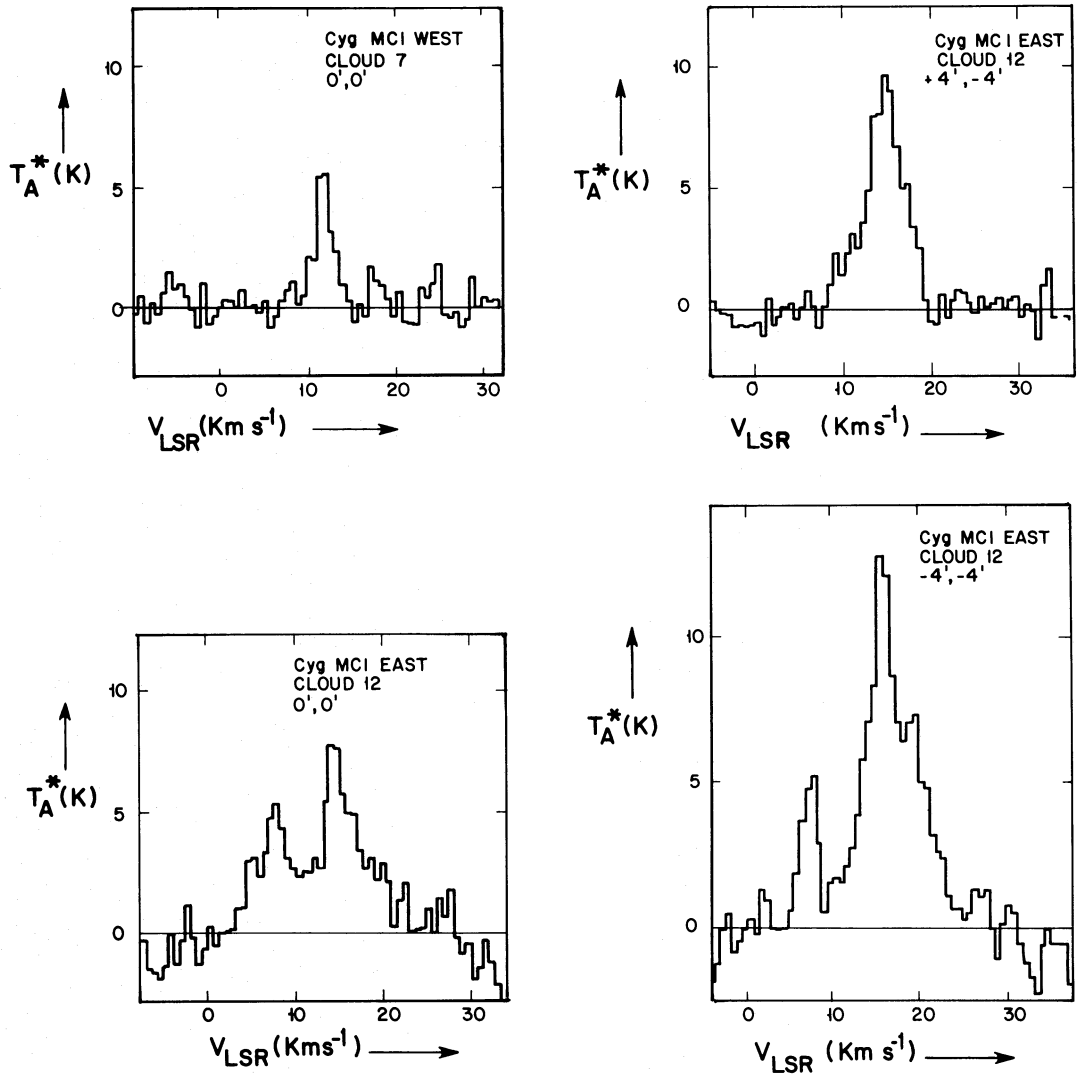


FIG. 11.—Some representative  $^{12}\text{CO}(1-0)$  profiles in the direction of clouds 7 and 12 (Table 1), observed with a 2/3 beam



(Matthews *et al.* 1977) and the far-infrared flux densities (Sargent *et al.* 1981) are consistent with the heating source being a single B0.5 star, or a tight cluster of a few later type B stars. In view of the compactness of the core and the large beamwidth used, the dust temperature  $T_d = 34$  K derived by Sargent *et al.* (1981) is almost certainly a lower limit. If the far-infrared source has the same dimensions as the molecular core, correction for beam dilution yields, for instance, a dust temperature  $T_d = 55$  K, which is typical for this kind of object. Likewise, the highest observed CO intensity  $T_A^* = 13$  K (implying  $T_k = 16$  K) must be a lower limit due to self-absorption. If  $T_d = T_k$  is assumed, the CO peak would be 70% absorbed. Such a high degree of self-absorption is consistent with the strong CO line broadening at the position of ON 1, and with the presence of  $\text{HCO}^+$  and  $\text{H}_2\text{CO}$  emission and absorption (Wootten, Snell, and Loren 1981; Forster, Goss, and Dickel 1981; this paper).

The ON 1 source complex thus shows the following characteristics.

1. It shows all the signs of recent star formation; the major heating source seems to be a *single* B0.5 star or at best a few later type B stars.

2. It is associated with a *compact* (size 1.2 pc) molecular cloud core with *high densities* [ $n(\text{H}_2)$  well in excess of  $10^4 - 10^5 \text{ cm}^{-3}$ ].

3. Only a *small part* of this cloud core shows direct evidence of interaction with the heating source: the OH maser,  $\text{H}_2\text{O}$  masers, H II region, and mid-infrared sources define an active region of size approximately 0.02 pc, whereas the full extent of the mid-infrared emission still defines a region not larger than 0.06 pc.

4. The characteristics of the dense core resemble those of cold clouds not associated with star formation. This may indicate that star formation in the ON 1 core is *very recent*, and that only part of the core is affected in a significant way.

5. In the Cyg MC1 West complex, no other signposts of star formation have been found so far, implying that ON 1 marks the *only site* of star formation in the complex. Again, this is unusual. (Signposts of star formation may, however, be present in the Cyg MC1 East complex.)

All these characteristics seem to imply that in the case of ON 1 we observe a molecular cloud complex at the very beginning of its star forming phase. ON 1 then is the *first* site of star formation in the complex, and it has turned on only *recently*. It is to be expected that contracting protostars that have not yet reached the nuclear burning stage may be hidden elsewhere in the cloud. This hypothesis can be verified by high resolution, high sensitivity far-infrared and molecular line observations.

Finally, a few words can be said about the mechanism of star formation in the ON 1 molecular cloud complex. Several mechanisms to induce molecular clouds to form

massive stars have been proposed; a convenient summary is given by Blitz (1980). In the case of ON 1, most mechanisms can be ruled out. Secondary star formation triggers such as the passage of an ionization shock, a supernova blast wave, or a stellar wind shell are not applicable in the absence of respectively other H II regions (Matthews *et al.* 1977), supernova remnants (unpublished WSRT observations), and OB associations (Humphreys 1978). A primary star formation trigger such as a cloud-cloud collision is likewise ruled out, since the present observations do not show any indication for this. Remaining possibilities are all primary mechanisms such as passing of a density wave, spontaneous (Jeans) collapse, or the presence of an accretion shock (Icke 1979).

## V. CONCLUSIONS

1. The ON 1 source complex is associated with an extended molecular cloud complex of overall dimensions  $25 \times 60$  pc at a distance of 1.4 kpc.

2. ON 1 is a site of star formation, exhibiting all the classical characteristics. It coincides with a compact core (size 1.2 pc) within a more extended envelope (size 5 pc).

3. CO,  $\text{H}_2\text{CO}$ , and  $\text{HCO}^+$  observations all indicate very high molecular densities [ $n(\text{H}_2) > 10^4 - 10^5 \text{ cm}^{-3}$ ] within the core. The central CO profiles are self-absorbed.

4. The molecular cloud core appears to be heated by a single B0.5 star, or at best a few close B stars. Only a small part of the core seems to be directly influenced by the heating source, indicating that it has turned on only recently, and that it has not yet had sufficient time to disrupt a sizable part of the core.

5. Apart from ON 1, the western part of the molecular cloud complex does not appear to have any other site of star formation. Some may exist in the eastern part of the complex. In any case, no signposts of star formation have been found within several pc of ON 1.

6. The apparent youth of ON 1 and its unusually isolated nature indicate that it marks the first site of star formation in the Cyg MC1 West complex, and thus marks the onset of star formation in this particular molecular cloud complex. The observations rule out several mechanisms for triggering star formation.

It is a pleasure to thank B. Baud, R. Genzel, and R. J. van Duinen for communicating observational results prior to publication, R. Loren for obtaining additional CO spectra. F. P. I. also acknowledges the warm support by P. Thaddeus, L. Blitz, H. Cong, and R. J. Cohen during part of these observations and thanks J. Bally for help in obtaining a high quality  $^{12}\text{CO}(1-0)$  spectrum of ON 1.

## REFERENCES

- Bally, J., and Lada, C. J. 1983, *Ap. J.*, **265**, 824.  
 Blitz, L. 1980, in *Giant Molecular Clouds in the Galaxy*, ed. P. M. Solomon and M. G. Edmunds (Oxford: Pergamon Press), p. 211.  
 Cato, B. T., Rönnäng, B. O., Rydbeck, O. E. H., Lewin, P. T., Yngvesson, K. S., Cardiasmenos, A. G., and Shanley, J. F. 1976, *Ap. J.*, **208**, 87.  
 Cohen, N. L. and Willson, R. F. 1981, *Astr. Ap.*, **96**, 230.  
 Davis, J. H. and Vanden Bout, P. 1973, *Ap. Letters*, **15**, 43.  
 Dickman, R. L. 1978, *Ap. J. Suppl.*, **37**, 407.  
 Downes, D., Genzel, R., Moran, J. M., Johnston, K. J., Matveyenko, L. I., Kogan, L. R., Kostenko, V. I., and Rönnäng, B. 1979, *Astr. Ap.*, **79**, 233.  
 Ellder, J., Rönnäng, B., and Winnberg, A. 1969, *Nature*, **223**, 67.  
 Forster, J. R., Goss, W. M., and Dickel, H. R. 1982, in *Regions of Recent Star Formation*, ed. R. S. Roger and P. E. Dewdney (Dordrecht: Reidel) p. 409.  
 Genzel, R., and Downes, D. 1977, *Astr. Ap. Suppl.*, **30**, 145.  
 Habing, H. J., and Israel, F. P. 1979, *Ann. Rev. Astr. Ap.*, **17**, 345.  
 Hardebeck, E. G. 1972, *Ap. J.*, **172**, 583.  
 Harris, S. 1974, *M.N.R.A.S.*, **166**, 29P.  
 Ho, P. T. P., Martin, R. N., and Barrett, A. H. 1981, *Ap. J.*, **246**, 761.  
 Hoessel, J. G., Elias, J. H., Wade, R. A., and Huchra, J. P. 1979, *Pub. A.S.P.*, **91**, 41.  
 Humphreys, R. M. 1978, *Ap. J. Suppl.*, **38**, 309.  
 Icke, V. 1979, *Astr. Ap.*, **78**, 352.  
 Israel, F. P. 1976, Ph.D. thesis, Leiden University.  
 Kutner, M. L., and Ulich, B. 1981, *Ap. J.*, **250**, 341.  
 Loren, R. B., and Wootten, A. 1980, *Ap. J.*, **242**, 568.  
 Lunel, M., Bergeat, J., Sibille, F., and Garnier, R. 1981, *M.N.R.A.S.*, **195**, 765.  
 Matthews, H. E., Goss, W. M., Winnberg, A., and Habing, H. J. 1977, *Astr. Ap.*, **61**, 261.  
 Morris, M., Palmer, P., Turner, B. E., and Zuckerman, B. 1974, *Ap. J.*, **191**, 349.  
 Rydbeck, O. E. H., Kollberg, E., Hjalmarson, A., Sime, A., Ellder, J., and Irvine, W. M. 1976, *Ap. J. Suppl.*, **31**, 333.  
 Sargent, A. I., van Duinen, R. J., Fridlund, C. V. M., Nordh, H. L., Aalders, and J. W. G. 1981, *Ap. J.*, **249**, 607.  
 Snell, R. 1981, *Ap. J. Suppl.*, **45**, 121.  
 Westerhout, G. 1969, *Maryland-Green Bank Galactic 21 cm Line Survey* (2d ed.; College Park, Md.: University of Maryland).  
 Winnberg, A., Habing, H. J., and Goss, W. M. 1973, *Nature Phys. Sci.*, **243**, 78.  
 Wootten, A., Loren, R., and Snell, R. 1982, *Ap. J.*, **255**, 160.  
 Wootten, A., Snell, R., and Evans, N. J. 1980, *Ap. J.*, **240**, 532.

F. P. ISRAEL: Astronomy Division, Space Science Department, ESTEC, Postbus 299, 2200 AG Noordwijk, The Netherlands

H. A. WOOTTEN: Department of Physics, Rensselaer Polytechnic Institute, Troy, NY 12181